Eur. Phys. J. C 2, 123–135 (1998)

THE EUROPEAN PHYSICAL JOURNAL C

Improved determination of the hadronic contribution to the muon $(g-2)$ and to $\alpha(M_Z^2)$ Using new data from hadronic τ decays

Ricard Alemany[1,a], Michel Davier[2,b], Andreas Höcker[2,c]

[1] CERN, CH-1211 Geneva 23, Switzerland (e-mail: alemany@alws.cern.ch)
[2] Laboratoire de l'Accélérateur Linéaire, IN2P3-CNRS et Université de Paris-Sud, F-91405 Orsay, France (e-mail: davier@lal.in2p3.fr, hoecker@lalcls.in2p3.fr)

Received: 6 March 1997

Abstract. We have reevaluated the hadronic contribution to the anomalous magnetic moment of the muon $(g-2)$ and to the running of the QED fine structure constant $\alpha(s)$ at $s = M_Z^2$. We incorporated new data from hadronic τ decays, recently published by the ALEPH Collaboration. In addition, compared to previous analyses, we use more extensive e^+e^- annihilation data sets. The integration over the total hadronic cross section is performed using experimental data up to 40 GeV and results from perturbative QCD above 40 GeV. The improvement from τ data concerns mainly the pion form factor, where the uncertainty in the corresponding integral could be reduced by more than a factor of two. We obtain for the lowest order hadronic vacuum polarization graph $a_\mu^{had} = (695.0 \pm 15.0) \times 10^{-10}$ and $\Delta\alpha^{(5)}_{had}(M_Z^2) = (280.9 \pm 6.3) \times 10^{-4}$ using e^+e^- data only. The corresponding results for combined e^+e^- and τ data are $a_\mu^{had} = (701.1 \pm 9.4) \times 10^{-10}$ and $\Delta\alpha^{(5)}_{had}(M_Z^2) = (281.7 \pm 6.2) \times 10^{-4}$, where the latter is calculated using the contribution from the five lightest quarks.

Introduction

The anomalous magnetic moment $a_\mu = (g-2)/2$ of the muon is experimentally and theoretically known to very high accuracy. In addition, the contribution of heavier objects to a_μ relative to the anomalous moment of the electron scales as $(m_\mu/m_e)^2 \sim 4 \times 10^4$. These properties allow an extremely sensitive test of the validity of QED and of additional contributions from strong and electroweak interactions. The present value from the combined μ^+ and μ^- measurements [1],

$$a_\mu \;=\; (11\,659\,230 \pm 85) \times 10^{-10} \;, \qquad (1)$$

should to be improved to a precision of at least 4×10^{-10} by a forthcoming Brookhaven experiment (BNL-E821) [2].

It is convenient to separate the prediction from the Standard Model (SM) a_μ^{SM} into its different contributions

$$a_\mu^{\rm SM} \;=\; a_\mu^{QED} + a_\mu^{had} + a_\mu^{weak} \;, \qquad (2)$$

where $a_\mu^{QED} = (11\,658\,470.6 \pm 0.2) \times 10^{-10}$ is the pure electromagnetic contribution (see [3] and references therein), a_μ^{had} is the contribution from hadronic vacuum polarization, and $a_\mu^{weak} = (15.1 \pm 0.4) \times 10^{-10}$ [3–5] accounts for corrections due to the exchange of the weak interacting bosons up to two loops[1]. Using the recent analysis of S. Eidelman and F. Jegerlehner[2] [7] that found a_μ^{had}(one-loop) $= (702.4 \pm 15.3) \times 10^{-10}$, and applying fourth order corrections due to the exchange of additional photons (incl. hadronic light-by-light scattering) and electron or quark loops, calculated by T. Kinoshita et al.[3] [9] to be $(-4.1 \pm 0.7) \times 10^{-10}$, one finds

$$a_\mu^{SM} = (11\,659\,184 \pm 16) \times 10^{-10} \;. \qquad (3)$$

Comparing the errors of the respective contributions to $a_\mu^{\rm SM}$ reveals that its total uncertainty is clearly dominated by the leading order vacuum polarization correction a_μ^{had}, originating from a quark-loop insertion into the muon vertex correction diagram as shown in Fig. 1.

In this letter, we present a new evaluation of the hadronic vacuum polarization contribution to a_μ and also to the running of the QED fine structure constant $\alpha(s)$ from low energy to the mass of the Z boson. In addition to using the complete and in comparison with previous analyses slightly enlarged experimental information on e^+e^- anni-

[1] The one-loop electroweak part of a_μ^{SM} with neglected Higgs boson contribution gives a_μ^{weak}(1 loop) $= 19.5 \times 10^{-10}$. Taking into account fermionic and bosonic two-loop corrections reduces the electroweak contribution to the value given in the text. The authors of [6] considered effects from non-zero quark

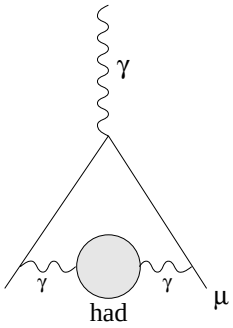

Fig. 1. Leading order hadronic vacuum polarization contribution to a_μ

hilation data, we incorporate new data from hadronic τ decays [10] which provide a more precise description of the hadronic contributions at energies less than 1.5 GeV. We bring attention to the straightforward and statistically well-defined averaging procedure and error propagation used in this paper, which takes into account full systematic correlations between the cross section measurements. We also stress our careful treatment of unmeasured final states which are bound via isospin constraints.

1 Hadronic vacuum polarization in γ and W propagators

As QCD is a non-Abelian theory with massless gauge bosons, its perturbative expansion at low energies is not well-behaved and non-perturbative effects lead to currently unpredictable long distance resonance phenomena in quark interactions. Fortunately, cross sections measured in e^+e^- annihilation and spectral functions from τ decays provide an experimental access to the hadronic vacuum polarization: from unitarity, the hadronic cross section of e^+e^- annihilation is related to the absorptive part of the vacuum polarization correlator via the optical theorem.

Similarly, hadronic spectral functions from τ decays are directly related to the isovector vacuum polarization currents when isospin invariance (CVC) and unitarity hold. For this purpose we have to worry whether the breakdown of CVC due to quark mass effects ($m_u \neq m_d$ generating $\partial_\mu J^\mu \sim (m_u - m_d)$ for a charge-changing hadronic current J^μ between u and d quarks) or unknown isospin-violating electromagnetic decays has non-negligible contributions within the present accuracy. Recent estimates of CVC predictions of τ branching ratios into vector final states [11] however show good agreement within about 5% experimental accuracy over the full range of exclusive vector hadronic final states. Expected deviations from CVC due to so-called *second class currents* as, *e.g.*, the decay $\tau^- \to \pi^-\eta\,\nu_\tau$ where the corresponding e^+e^- final state $\pi^0\eta$ (C=+1) is strictly forbidden, have estimated branching fractions of order of $(m_u - m_d)^2 \simeq 10^{-5}$ [12], while the experimental upper limit amounts to $\mathrm{B}(\tau \to \pi^-\eta\,\nu_\tau) < 1.4 \times 10^{-4}$ [13] with 95% CL. Another classical test is the pion β-decay, yielding a sensitivity to CVC violation of 3%. The CVC hypothesis relates the isovector, vector matrix element of the decay $\pi^- \to \pi^0 e^- \bar{\nu}_e$ to the electromagnetic form factor of the pion. No deviation between the CVC branching ratio and the experimental result has been found [14,13].

An estimate of a possible CVC violation can be obtained in the $\pi\pi$ final state which is dominated by the $\rho(770)$ resonance. $SU(2)$ symmetry breaking can occur in the $\rho^\pm$–ρ^0 masses and widths caused by electromagnetic interactions. Hadronic contributions to the $\rho^\pm$–ρ^0 width difference are expected to be much smaller since they are proportional to $(m_u - m_d)^2$. The different electromagnetic contributions to the width are listed in Table 1: radiative transitions introduce a negligible effect, while the dominant contribution comes from the $\pi^\pm$–π^0 mass difference. A recent theoretical analysis [16] indicates that the $\rho^\pm$ and ρ^0 masses are in fact equal within 0.5 MeV/c^2: $m_{\rho^\pm} - m_{\rho^0} = -(0.15 \pm 0.55)$ MeV/c^2. This prediction has been verified in the ALEPH analysis of the τ vector spectral functions [10] with the result: $m_{\rho^\pm} - m_{\rho^0} = -(0.0 \pm 1.0)$ MeV/c^2. Since the π^- and π^0 mass difference is known experimentally [13] to be $m_{\pi^\pm} - m_{\pi^0} = (4.5936 \pm 0.0005)$ MeV/c^2 and understood theoretically [17] to be almost completely from electromagnetic origin, it is expected that the total $\rho^\pm$ and ρ^0 widths should be different even in the limit where hadronic interactions are $SU(2)$-invariant (this includes the chiral limit). An additional point concerns contributions from photon bremsstrahlung. While the infrared divergences in $\rho \to \pi\pi\gamma$ decays vanishes when including the vertex correction graphs, finite terms are expected to contribute differently to the widths of the charged and the neutral ρ. The corresponding bremsstrahlung graphs have been calculated in [15]. The width contributions from finite terms to both the $\rho^\pm$ and the ρ^0 turn out to be negative. The estimate of the width difference given in Table 1 assumes finite contributions to the widths from loop corrections to be small.

The total expected $SU(2)$ violation in the ρ width is finally computed from the above considerations to be

$$\frac{\Gamma_{\rho^\pm} - \Gamma_{\rho^0}}{\Gamma_\rho} \;=\; (2.8 \pm 3.9) \times 10^{-3}\;, \qquad (4)$$

where the error comes essentially from the estimate of the $\rho^\pm$–ρ^0 mass difference and of the $\pi\pi\gamma$ contribution. This effect introduces corrections for a_μ^{had} and the running of $\alpha(s)$ when including τ data (see Sect. 6).

From a more qualitative point of view, one should keep in mind that in this analysis the CVC hypothesis is applied at a very low energy scale where the absorptive parts of the matrix elements are largely dominated by non-perturbative QCD which are expected to factorize from their respective W or γ excitation.

masses and obtained $\Delta a_\mu^{weak}(2\text{ loop}) \simeq -(36.9 \pm 2.5) \times 10^{-11}$, which gives $a_\mu^{weak} = 15.8 \times 10^{-10}$

[2] Historically, the first evaluation of the hadronic vacuum polarization contribution to the muon $(g-2)$ was performed in [8]

[3] For a discussion of the higher order contributions considered in this analysis see Sect. 6.2

Table 1. Expected CVC violation from electromagnetic interactions in $\rho^{\pm}$–ρ^0 decays

Final states	$\frac{\Gamma_{\rho^\pm}-\Gamma_{\rho^0}}{\Gamma_\rho}$ $(\times 10^3)$	Ref.
$\pi\omega \to \pi\pi^0\gamma$	0.32	[15]
$\pi\gamma$	-0.34 ± 0.21	[13]
$\eta\gamma$	-0.38 ± 0.07	[13]
$\ell^+\ell^-$	-0.091 ± 0.004	[13]
$m_{\pi^\pm} - m_{\pi^0}$, $m_{\rho^\pm} - m_{\rho^0}$	6.3 ± 2.5	[13,16]
$\pi\pi\gamma$	-3 ± 3	[15]
Sum	2.8 ± 3.9	

However, electroweak radiative corrections must be taken into account. Their dominant contribution comes from the short distance correction to the effective four-fermion coupling $\tau^- \to (d\bar{u})^- \nu_\tau$ yielding the fractional logarithmic term $(\alpha(M_\tau)/2\pi)(4\ln(M_{\rm Z}/M_\tau) + 5/6)$ [18] which vanishes in leptonic τ decays. The short distance correction can be absorbed into an overall multiplicative electroweak correction $S_{\rm EW}$ introduced in the definition of the spectral functions used in [10]. The resummation of higher-order electroweak logarithms using the renormalization group yields [19,20]

$$S_{\rm EW} = \left(\frac{\alpha(m_b)}{\alpha(M_\tau)}\right)^{\frac{9}{19}} \times \left(\frac{\alpha(M_{\rm W})}{\alpha(m_b)}\right)^{\frac{9}{20}} \times \left(\frac{\alpha(M_{\rm Z})}{\alpha(M_{\rm W})}\right)^{\frac{36}{17}} = 1.0194\,, \quad (5)$$

while remaining perturbative electroweak corrections are of order $\alpha^n(M_\tau)\ln^n(M_{\rm Z}/M_\tau)$ which is safe to ignore. The subleading non-logarithmic short distance correction, calculated to order $O(\alpha)$ at quark level: $5\alpha(M_\tau)/12\pi \simeq 0.0010$ [18] turns out to be small. Additional long-distance corrections are expected to be final state dependent. They have only been computed for the $\tau^- \to \pi^-\nu_\tau$ decay leading to a total radiative correction of 2.03% [21] which is dominated by the leading logarithm from the short distance contribution. The evaluation of (5) neglects radiative corrections from additional gluon exchange between the final state quarks.

To be safe [22], the uncertainty of $S_{\rm EW}$ in (5) is estimated to be $\Delta S_{\rm EW} = 0.0040$, which is taken into account in the CVC cross section prediction from τ decays.

1.1 Muon magnetic anomaly

By virtue of the analyticity of the vacuum polarization correlator, the contribution of the hadronic vacuum polarization to a_μ can be calculated via the dispersion integral [23]

$$a_\mu^{had} = \frac{1}{4\pi^3}\int_{4m_\pi^2}^{\infty} ds\,\sigma_{had}(s)\,K(s)\,. \quad (6)$$

Here $\sigma_{had}(s)$ is the total $e^+e^- \to$ hadrons cross section as a function of the c.m. energy-squared s, and $K(s)$ denotes the QED kernel [24]

$$K(s) = x^2\left(1-\frac{x^2}{2}\right) + (1+x)^2\left(1+\frac{1}{x^2}\right) \times \left(\ln(1+x) - x + \frac{x^2}{2}\right) + \frac{(1+x)}{(1-x)}x^2\ln x \quad (7)$$

with $x = (1-\beta_\mu)/(1+\beta_\mu)$ and $\beta = (1-4m_\mu^2/s)^{1/2}$ (see also remarks concerning the numerical stability of $K(s)$ in [7]). The function $K(s)$ decreases monotonically with increasing s. It gives a strong weight to the low energy part of the integral (6). About 91% of the total contribution to a_μ^{had} is accumulated at c.m. energies $\sqrt{s}$ below 2.1 GeV while 72% of a_μ^{had} is covered by the two-pion final state which is dominated by the $\rho(770)$ resonance. Recent τ data published by the ALEPH Collaboration provide a very precise spectrum of the two-pion final state as well as new input for the more controversial four-pion final states. This new information can significantly improve the a_μ^{had} determination.

1.2 Running of the QED fine structure constant

In the same spirit we evaluate the hadronic contribution $\Delta\alpha_{\rm had}(s)$ to the renormalized vacuum polarization function $\Pi'_\gamma(s)$ which governs the running of the electromagnetic fine structure constant $\alpha(s)$. For the spin 1 photon, $\Pi'_\gamma(s)$ is given by the Fourier transform of the contraction of the electromagnetic currents $j^\mu_{em}(s)$ in the vacuum $(q^\mu q^\nu - q^2 g^{\mu\nu})\,\Pi'_\gamma(q^2) = i\int d^4x\, e^{iqx}\langle 0|T(j^\mu_{em}(x) j^\nu_{em}(0))|0\rangle$. With $\Delta\alpha(s) = -4\pi\alpha\,{\rm Re}\left[\Pi'_\gamma(s) - \Pi'_\gamma(0)\right]$, one has

$$\alpha(s) = \frac{\alpha(0)}{1-\Delta\alpha(s)}\,, \quad (8)$$

where $4\pi\alpha(0)$ is the square of the electron charge in the long-wavelength Thomson limit. The contribution $\Delta\alpha(s)$ can naturally be subdivided in a leptonic and a hadronic part. Furthermore, at $s = M_{\rm Z}^2$ it is appropriate to separate the leading vacuum polarization contribution involving the five light quarks u, d, s, c, b from the top quark contribution since the latter cannot be calculated in the light fermion approximation.

The leading order leptonic contribution is given by

$$\Delta\alpha_{\rm lep}(M_{\rm Z}^2) = \frac{\alpha(0)}{3\pi}\sum_\ell\left(\ln\frac{M_{\rm Z}}{m_\ell^2} - \frac{5}{3}\right) = 314.2\times 10^{-4}. \quad (9)$$

Using analyticity and unitarity, the dispersion integral for the contribution from the light quark hadronic vacuum polarization $\Delta\alpha^{(5)}_{\rm had}(M_{\rm Z}^2)$ reads [25]

$$\Delta\alpha^{(5)}_{\rm had}(M_{\rm Z}^2) = -\frac{M_{\rm Z}^2}{4\pi^2\,\alpha}\,{\rm Re}\int_{4m_\pi^2}^{\infty} ds\,\frac{\sigma_{had}(s)}{s - M_{\rm Z}^2 - i\epsilon}\,, \quad (10)$$

where $\sigma(s) = 16\pi^2\alpha^2(s)/s \cdot \mathrm{Im}\Pi'_\gamma(s)$ from the optical theorem, and $\mathrm{Im}\Pi'_\gamma$ stands for the absorptive part of the hadronic vacuum polarization correlator. In contrast to a_μ^{had}, the integration kernel favours cross sections at higher masses. Hence, the improvement when including τ data is expected to be small.

The top quark contribution can be calculated using the next-to-next-to-leading order α_s^3 prediction of the total inclusive cross section ratio R, defined as

$$R(s) \;=\; \frac{\sigma_{tot}(e^+e^- \to \mathrm{h}adrons)}{\sigma(e^+e^- \to \mu^+\mu^-)} \;=\; \frac{3s}{4\pi\alpha^2}\sigma_{tot}\;, \qquad (11)$$

from perturbative QCD [26,7]:

$$R_{\mathrm{pert}}(s) = 3\sum_f Q_f^2 \left(1 - \frac{4m_f^2}{s}\right)^{1/2}\left(1 + \frac{2m_f^2}{s}\right) \left[1 + \frac{\alpha_s}{\pi} + r_1\left(\frac{\alpha_s}{\pi}\right)^2 + r_2\left(\frac{\alpha_s}{\pi}\right)^3\right]\;, \qquad (12)$$

where $r_1 = 1.9857 - 0.1153\,n_f$, $r_2 = -6.6368 - 1.2001\,n_f - 1.2395(\sum_f Q_f)^2/3\sum_f Q_f^2$ and n_f is the number of involved quark flavours. The evaluation of the integral (10) with $m_{top} = 175$ GeV and the running strong coupling constant fixed at $\alpha_s(M_\mathrm{Z}^2) = 0.121$ yields $\Delta\alpha_{top}(M_\mathrm{Z}^2) = -0.6 \times 10^{-4}$.

Using $\Delta\alpha^{(5)}_{had}(M_\mathrm{Z}^2) = (280 \pm 7) \times 10^{-4}$ [7], one obtains

$$\alpha^{-1}(M_\mathrm{Z}^2) \;=\; 128.902 \pm 0.090\;. \qquad (13)$$

Again, the error is dominated by the hadronic vacuum polarization part that is not calculable within perturbative QCD.

2 The integration procedure

The information used for the evaluation of the integrals (6) and (10) comes mainly from direct measurements of the cross sections in e^+e^- annihilation and via CVC from τ spectral functions. The integrals themselves are evaluated using the trapezoidal rule, *i.e.*, combining adjacent measurement points by straight lines. Even if this method is straightforward and free from theoretical constraints (other than CVC in the τ case), its numerical calculation requires special care. The combination of measurements from different experiments taking into account correlations – both inside each data set and between different experiments are subjected to additional studies and discussions.

2.1 Averaging data from different experiments

In order to exploit the maximum information, we combine weighted measurements of different experiments at a given energy instead of calculating separately the integrals for every experiment and finally averaging them[4]. Generally, if different measurements at a given c.m. energy show inconsistencies, *i.e.*, their χ^2 per degree of freedom (dof) is larger than one, we rescale the error of their weighted average with $\sqrt{\chi^2/\mathrm{d}o\!f}$.

The solution of the averaging problem is found using a correlated χ^2 minimization. We define

$$\chi^2 \;=\; \sum_{n=1}^{N_{exp}}\sum_{i,j=1}^{N_n}(x_i^n - k_i)\,(C_{ij}^n)^{-1}\,(x_j^n - k_j)\;, \qquad (14)$$

where x_i^n is the ith cross section measurement of the nth experiment in a given final state, C_{ij}^n is the covariance between the ith and the jth measurement and k_i is the unknown distribution. The covariance matrix C^n is defined as

$$C_{ij}^n = \begin{cases} (\Delta_{i,stat}^n)^2 + (\Delta_{i,sys}^n)^2 & for\ i = j \\ \Delta_{i,sys}^n \cdot \Delta_{j,sys}^n & for\ i \neq j \end{cases}\;, \quad i,j = 1,\ldots,N_n\;, \qquad (15)$$

where $\Delta_{i,stat}^n$ ($\Delta_{i,sys}^n$) denotes the statistical (systematic) error of x_i^n. The systematic errors of the e^+e^- annihilation measurements are essentially due to luminosity and efficiency uncertainties. The minimum condition $d\chi^2/dk_i = 0,\ \forall i$ leads to the linear equation problem

$$\sum_{n=1}^{N_{exp}}\sum_{j=1}^{N_n}(x_j^n - k_j)\,(C_{ij}^n)^{-1} \;=\; 0\;, \quad i = 1,\ldots,N_n\;. \qquad (16)$$

The inverse covariance $\tilde{C}_{ij}^{-1}$ between the solutions k_i, k_j is the sum over the inverse covariances of every experiment

$$\tilde{C}_{ij}^{-1} \;=\; \sum_{n=1}^{N_{exp}}(C_{ij}^n)^{-1}\;. \qquad (17)$$

2.2 Correlations between experiments

Equation (17) provides the covariance matrix needed for the error propagation when calculating the integrals over the solutions k_i from (16). Up to this point, $\tilde{C}_{ij}$ only contains correlations between the systematic uncertainties within the same experiment. However, due to commonly used simulation techniques for acceptance and luminosity determinations as well as state-of-the-art calculations of radiative corrections, systematic correlations from one

[4] One could imagine two experiments a and b, each with two independent measurements $a_1(E_1) \pm \Delta a_1$, $a_2(E_2) \pm \Delta a_2$ and $b_1(E_1) \pm \Delta b_1$, $b_2(E_2) \pm \Delta b_2$ at energies $E_1 \neq E_2$. Setting $\Delta a_1 = \Delta a_2 = \Delta b_1 = \Delta b_2$ leads to identical errors in both integration methods. However, non-symmetric errors as, *e.g.*, $\Delta a_1/2 = 2\Delta a_2 = 2\Delta b_1 = \Delta b_2/2$ propagate a 53% larger uncertainty when calculating independently the sum over the points (trivial integration) of the experiments a, b and averaging afterwards rather than averaging $\langle a_1, b_1\rangle$ and $\langle a_2, b_2\rangle$ first, *i.e.*, keeping the energy information of the respective points in the average

experiment to another cannot be excluded. It is clearly a difficult task to reasonably estimate the amount of such correlations as they depend on the capabilities of the contributing experiments and one's theoretical understanding of the dynamics of the respective final states. In general, one can state that in older experiments, where only parts of the total solid angle were covered by the detector acceptance, individual experimental limitations should dominate the systematic uncertainties. Potentially common systematics, such as radiative corrections or efficiency, acceptance and luminosity calculations based on the Monte Carlo simulation, play only minor roles. The correlations between systematic errors below 2 GeV c.m. energy are therefore estimated to be between 10% and 30%, with the exception of the $\pi^+\pi^-$ final state, where we impose a 40% correlation due to the easier experimental situation and the better knowledge of the dynamics which leads to non-negligible systematic contributions from the uncertainties of the radiative corrections. At energies above 2.1 GeV the experiments measured the total inclusive cross section ratio R. Between 2.1 and 3.1 GeV, individual technical problems dominate the systematic uncertainties. At higher energies, new experiments provide nearly full geometrical acceptance which decreases the uncertainty of efficiency estimations. Radiative corrections as well as theoretical errors of the luminosity determination give important contributions to the final systematic errors quoted by the experiments. We therefore estimate the correlations between the systematic errors of the experiments to be negligible between 2 GeV and 3 GeV, 20% between 3 GeV and 10 GeV, and 30% above 10 GeV.

These correlation coefficients are added to all those entries of $\tilde{C}_{ij}$ from (17) which involve two different experiments.

2.3 Inclusion of τ data

In this analysis we include additional data from τ decays into two- and four-pion final states[5]: $\tau^- \to \pi^-\pi^0\,\nu_\tau$, $\tau^- \to \pi^- 3\pi^0\,\nu_\tau$ and $\tau^- \to 2\pi^-\pi^+\pi^0\,\nu_\tau$, recently published by the ALEPH Collaboration [10]. Assuming isospin invariance to hold, the corresponding e^+e^- isovector cross sections are calculated via the CVC relations

$$\sigma^{I=1}_{e^+e^-\to\pi^+\pi^-} = \frac{4\pi\alpha^2}{s}\, v_{1,\,\pi^-\pi^0\,\nu_\tau}\ , \tag{18}$$

$$\sigma^{I=1}_{e^+e^-\to\pi^+\pi^-\pi^+\pi^-} = 2\cdot\frac{4\pi\alpha^2}{s}\, v_{1,\,\pi^- 3\pi^0\,\nu_\tau}\ , \tag{19}$$

$$\sigma^{I=1}_{e^+e^-\to\pi^+\pi^-\pi^0\pi^0} = \frac{4\pi\alpha^2}{s}\left[v_{1,\,2\pi^-\pi^+\pi^0\,\nu_\tau} - v_{1,\,\pi^- 3\pi^0\,\nu_\tau}\right]\ . \tag{20}$$

The τ spectral functions v_1 are given as binned continous distributions of the mass-squared s. In each bin i, the spectral function $v_1(s_i)$ contains the (normalized) invariant mass spectrum $\Delta N_i/N$, integrated over the bin width ds_i. On the contrary e^+e^- cross sections are measured at discrete energy settings. To each e^+e^- measurement is associated a τ cross section value obtained by interpolating between adjacent bins. This interpolation takes into account the correlations between the bins and is achieved imposing a functional form obtained from a fit to Breit-Wigner resonances [10] using the Gounaris-Sakurai parametrization [28]. However, the fit function is renormalized in each bin so that its integral over the width of each bin corresponds to the measured CVC cross section for that bin. All the data points – τ, e^+e^- and interpolated τ values – are injected with their correlations into (16) and (17).

Due to the high bin-to-bin correlations of the τ data and the significant normalization uncertainty coming from the τ hadronic branching ratios, biases of the least-square minimization [27] cannot be excluded. We therefore calculate the average solution twice, *i.e.*, with and without correlations, use the mean value of both integrations as the result and add half of the total difference as additional systematic error. This is done in all cases where τ data are involved. The effect amounts to about 10% of the total error.

2.4 Evaluation of the integral

The procedure described above provides the weighted average and the covariance of the cross sections from different experiments contributing to a certain final state in a given range of c.m. energies. We now apply the trapezoidal rule. In order to perform the integrations (6) and (10), we subdivide the integration range in sufficiently small energy steps and calculate for each of these steps the corresponding covariance (where additional correlations induced by the trapezoidal rule have to be taken into account). This procedure yields error envelopes between adjacent measurements as depicted by the shaded bands in Figs. 2 and 3.

3 Radiative corrections

Higher order radiative corrections bias the measurements of both cross sections in e^+e^- annihilation and invariant mass spectra from τ hadronic decays. The e^+e^- experiments generally correct the measured cross section for QED effects, including bremsstrahlung, vacuum polarization and higher order self-energy graphs (see references in [7]). Following the prescription of [7], we have multiplied all inclusive cross section measurements R at masses below the J/ψ resonance by the (small) correction factor $(1+\Delta\alpha_{\rm lep}(s))(\alpha/\alpha(s))^2$ in order to account for the missing correction for hadronic vacuum polarization.

In τ decays, final state radiation from the τ itself or from its decay products can influence the invariant mass measurement. Due to the high mass of the τ lepton, the bremsstrahlung graph is largely suppressed. Both types of radiation are included in the Monte Carlo simulation program KORALZ [29], used by ALEPH to unfold the measured distributions from detector resolution and physical

[5] Throughout this paper, charge conjugate states are implied

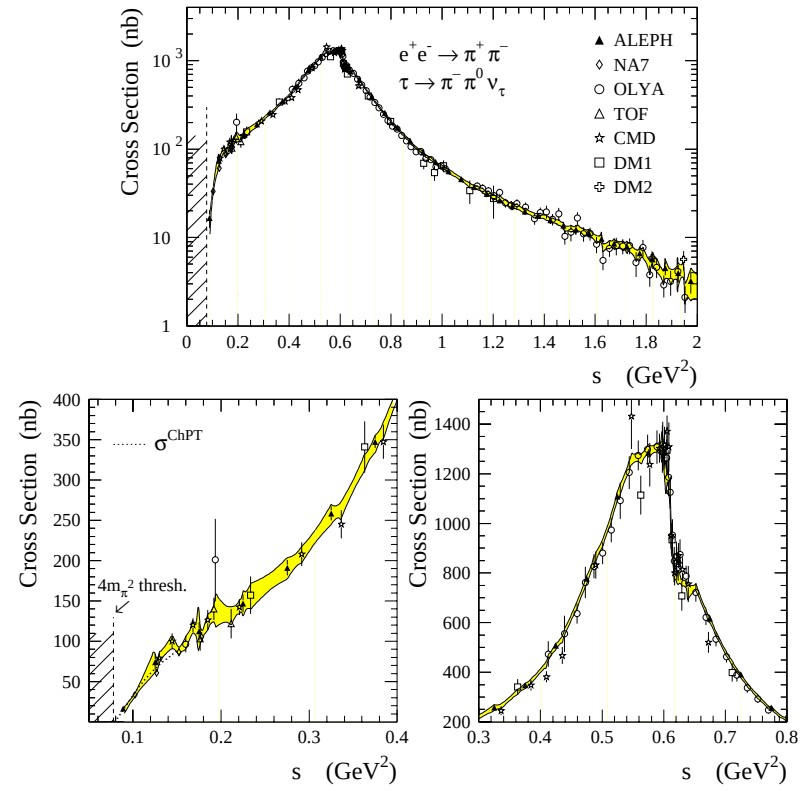

Fig. 2. Two-pion cross section as a function of the c.m. energy-squared. The *band* represents the result of the averaging procedure described in the text within its diagonal errors. The *lower left hand plot* shows the chiral expansion of the two-pion cross section obtained from expression (21)

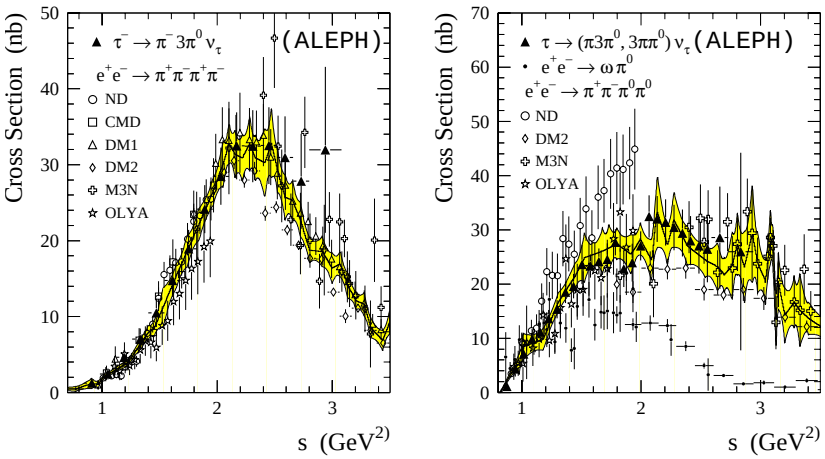

Fig. 3. Four-pion cross section as a function of the c.m. energy-squared. The band represents the result of the averaging procedure described in the text within its diagonal errors. The *right-hand plot* shows additionally the $e^+e^- \to \omega\pi^0$ amplitude (*small points*)

(higher order) effects. Even if the actual frequency with which final state radiation occurs or if its energy were not well simulated in the Monte Carlo, reconstructed photons found to originate from radiation of the τ decay [30] are included in the invariant mass determination, and thus do not bias the measurement.

Electroweak radiative corrections are applied through the CVC correction factor S_{EW} defined in (5).

4 The origin of the data

The exclusive low energy e^+e^- cross sections have mainly been measured by experiments working at e^+e^- colliders in Novosibirsk and Orsay. Due to the high hadron multiplicity at energies above 2.5–3.1 GeV, the exclusive measurement of the respective hadronic final states is not practicable. Consequently, the experiments at the high energy colliders DORIS and PETRA (DESY) and PEP (SLAC) have measured the total inclusive cross section ratio R.

We give in the following a compilation of the data used in this analysis:

- The $e^+e^-\to\pi^+\pi^-$ measurements are taken from OLYA [31,32], TOF [33], NA7 [34], CMD [31], DM1 [35] and DM2 [36]. In addition, we use τ data from ALEPH [10] normalized to the world average branching ratio $\mathrm{B}(\tau^-\to\pi^-\pi^0\,\nu_\tau)=(25.24\pm0.16)\%$[13]. According to (18), τ data provide only the dominant isovector part of the total two-pion cross section. A correction due to the small isospin-violating isoscalar $\omega\to\pi^+\pi^-$ final state, which interferes with the isovector amplitude, is applied. A small correction for the missing, *i.e.*, unmeasured decay modes $\rho\to\pi^0\gamma$ (only for e^+e^- data) and $\rho\to\ \eta\gamma$, is added.
- The reaction $e^+e^-\to\pi^+\pi^-\pi^0$ is dominated by the ω and ϕ intermediate resonances. In the peak region of these resonances we use analytic parametrizations of the cross sections. The non-resonant data are taken from ND [37], M2N [38], M3N [39], DM1 [40] and DM2 [41]. Corrections for the missing ω and ϕ decay modes are applied.
- The $e^+e^-\to\pi^+\pi^-\pi^0\pi^0$ data are available from OLYA [42], ND [37], M2N [38], DM2 [43–46] and M3N [39]. According to (20), a linear combination of both four-pion τ decay channels measured by ALEPH [10] connects the corresponding spectral functions with the above e^+e^- final state. We use the two branching ratios $\mathrm{B}(\tau^-\to2\pi^-\pi^+\pi^0\,\nu_\tau)=(4.25\pm0.09)\%$ and $\mathrm{B}(\tau^-\to\pi^-3\pi^0\,\nu_\tau)=(1.14\pm0.14)\%$[13], as an appropriate normalization.
- The reaction $e^+e^-\to\ \omega\pi^0$ is mainly reconstructed in the $\pi^+\pi^-\pi^0\pi^0$ final state. It was studied by the collaborations ND [37] and DM2 [45]. Corrections for the missing ω decay modes are applied.
- The $e^+e^-\to\ \pi^+\pi^-\pi^+\pi^-$ final state was studied by the experiments OLYA [42], ND [37], MEA [47], CMD [48], DM1 [49,50], DM2 [43,45,46] and M3N [39]. The corresponding spectral function from $\tau^-\to\pi^-3\pi^0\,\nu_\tau$ (according to (19)) is provided by ALEPH [10].
- The $e^+e^-\to\ \pi^+\pi^-\pi^+\pi^-\pi^0$ final state is taken from M3N [39] and CMD [48]. The other five-pion mode $e^+e^-\to\pi^+\pi^-3\pi^0$ can be accounted for using the rigourous isospin relation $\sigma_{\pi^+\pi^-3\pi^0}=0.5\times\sigma_{\pi^+\pi^-\pi^+\pi^-\pi^0}$.
- For the reaction $e^+e^-\to\ \omega\pi^+\pi^-$, measured by the groups DM1 [49] and DM2 [48], a correction for ω decays other than into three pions which appear in the five-pion final state is applied.
- The $e^+e^-\to\ \pi^+\pi^-\eta$ data were studied by ND [37] and DM2 [51]. We subtract from the cross section the contributions which are already counted in the $\pi^+\pi^-\pi^+\pi^-\pi^0$ and $\pi^+\pi^-3\pi^0$ finale states.
- The cross sections of the six-pion final states $3\pi^+3\pi^-$ and $2\pi^+2\pi^-2\pi^0$ were measured by DM1 [52], M3N [39] CMD [48] and DM2 [44]. In [10] an upper limit for the unknown $\pi^-\pi^+\,4\pi^0$ cross section of $\sigma_{\pi^+\pi-4\pi^0}\le(3/2)\times\sigma_{2\pi^-2\pi^+\,2\pi^0}-(9/24)\times\sigma_{3\pi^-3\pi^+}$ was derived using isospin constraints. We take half of this upper limit as the estimated contribution, with an error of 100%.
- The $e^+e^-\to\mathrm{K}^+\mathrm{K}^-$ and $e^+e^-\to\mathrm{K}^0_\mathrm{S}\mathrm{K}^0_\mathrm{L}$ cross sections are taken from OLYA [53], DM1 [54] and DM2 [55].
- The reactions $e^+e^-\to\mathrm{K}^0_\mathrm{S}\,\mathrm{K}^+\pi^-$ and $e^+e^-\to\mathrm{K}^+\mathrm{K}^-\pi^0$ were studied by DM1 [56,57] and DM2 [43]. Using isospin symmetry the cross section of the final state $\mathrm{K}^0_\mathrm{S}\mathrm{K}^0_\mathrm{L}\pi^0$ is obtained from the relation $\sigma_{\mathrm{K}^0_\mathrm{S}\mathrm{K}^0_\mathrm{L}\pi^0}=\sigma_{\mathrm{K}^+\mathrm{K}^-\pi^0}$.
- The inclusive reaction $e^+e^-\to\mathrm{K}^0_\mathrm{S}+X$ was analyzed by DM1 [58]. After subtracting from its cross section the separately measured contributions of the final states $\mathrm{K}^0_\mathrm{S}\mathrm{K}^0_\mathrm{L}$, $\mathrm{K}^0_\mathrm{S}\,\mathrm{K}^+\pi^-$ and $\mathrm{K}^0_\mathrm{S}\mathrm{K}^0_\mathrm{L}\pi^0$, it still includes the modes $\mathrm{K}^0_\mathrm{S}\mathrm{K}^0_\mathrm{S}\pi^+\pi^-$, $\mathrm{K}^0_\mathrm{S}\mathrm{K}^0_\mathrm{L}\pi^+\pi^-$, $\mathrm{K}^0_\mathrm{S}\mathrm{K}^+\pi^-\pi^0$ and $\mathrm{K}^0_\mathrm{S}\mathrm{K}^-\pi^+\pi^0$. With the assumption that the cross sections for the processes $e^+e^-\to\mathrm{K}^0\bar{\mathrm{K}}^0(\pi\pi)^0$ and $e^+e^-\to\mathrm{K}^+\mathrm{K}^-(\pi\pi)^0$ are equal, one can summarize the total $\mathrm{K}\bar{\mathrm{K}}\pi\pi$ contribution as twice the above corrected $\mathrm{K}^0_\mathrm{S}+X$ cross section. A reasonable estimate of the systematic uncertainty, implied by the assumption made, is obtained by taking the cross section for the channel $\mathrm{K}^+\mathrm{K}^-\pi^+\pi^-$ measured by DM1 [56] and DM2 [43].
- At higher energy the total cross section ratio R is measured inclusively. We use the data provided by the experiments $\gamma\gamma2$ [59], MARK I [60], DELCO [61], DASP [62], PLUTO [63], LENA [64], Crystal Ball [65], MD-1 [66], CELLO [67], JADE [68], MARK-J [69], TASSO [70], CLEO [71], CUSB [72] and MAC [73]. Above 3.5 GeV the measurements of the MARK I Collaboration are significantly higher than those from LENA, PLUTO and Crystal Ball. In addition, the QCD prediction of R, which should be reliable in this energy regime, favours lower values. In agreement with [7], we neglect MARK I data above this energy threshold.

  Although small, the enhancement of the cross section due to γ–Z interference is corrected for c.m. energies above the J/ψ mass. We use a factorial ansatz according to [74,7], yielding a negligible contribution to a_μ^{had} and a -0.30×10^{-4} shift of $\Delta\alpha^{(5)}_{had}(M_\mathrm{Z}^2)$.

5 Analytical contributions

In some energy regions where data information is scarce and/or reliable theoretical predictions are available, we use analytical contributions to extend the experimental integral.

5.1 The $\pi^+\pi^-$ threshold region

To overcome the lack of data at threshold energies, a second order expansion obtained from *Chiral Perturbation Theory* [75] is used as a description of the pion form factor F_π (which is connected with the two-pion cross section via the expression $|F_\pi|^2=3s\sigma_{\pi\pi}/(\pi\alpha^2(1-4m_\pi^2/s)^{3/2})$:

$$F_\pi^{ChPT}\ \simeq\ 1+\frac{1}{6}\langle r^2\rangle_\pi\,s+c_\pi\,s^2+O(s^3)\ . \qquad (21)$$

Exploiting precise results from space-like data [76], the pion charge radius-squared $\langle r^2\rangle_\pi=(0.431\ \pm\ 0.026)\ \mathrm{fm}^2$ and the coefficient $c_\pi=(3.2\pm1.0)\ \mathrm{GeV}^{-4}$ from (21) have recently been determined [77] by means of a simultaneous fit.

5.2 Narrow resonances

The e^+e^- annihilation cross section involves narrow resonances such as the $\omega(782)$ and $\phi(1020)$ at low energies, the J/ψ and Υ resonances at the $c\bar{c}$ and $b\bar{b}$ quark thresholds, respectively, as well as their excited spectroscopic states. It is safe to parametrize these states using relativistic Breit-Wigner resonance shapes with an s-dependent width. We use the formulae given in [7]. The physical input values of the parametrizations and their errors are taken from [13]. The total parametrization errors are then calculated by gaussian error propagation.

5.3 High energy tail

At energies sufficiently above the Υ resonance family, the perturbative QCD prediction of R with five active quarks is supposed to be reliable. In agreement with [7] we use $R_{\rm pert}(s)$ from (12) for $\sqrt{s} \geq 40$ GeV.

6 Results

We evaluate the integrals (6) and (10) exclusively, *i.e.*, for every contributing final state, up to the c.m. energy of 2.125 GeV. Even if some particular modes have been measured up to somewhat higher energies, we have to worry about unmeasured exclusive modes and therefore use the total R measurement above this threshold. Both energy regions are assumed to be uncorrelated. Because the contributions of the exclusive channels at low energy are simply summed up, we have to estimate their respective covariances when propagating the error: in general, unmeasured final states whose contributions are deduced from measured ones via isospin are set to be 100% correlated with these. Also different detectors performing the same measurement are correlated through the sharing of commonly used simulation techniques to calculate acceptance and selection efficiency which depend on the assumed underlying physical dynamics. Contributions from resonances that are analytic are globally assumed to have 20% correlations due to modelling uncertainties. Between purely measured final states we have estimated the correlations depending on the number of common experiments that contribute to their measurements and on the common energy region, as well as according to the relative importance of their statistical and systematic errors. In general our estimation yields a correlation between 10% and 20%. This treatment is different from that of [78] where a 100% correlation was assumed.

As described in Sect. 1, corrections to the charged $\rho^\pm$ width have to be applied to account for small CVC-violating effects. The magnitude of the width difference (4) translated into $a_\mu^{\rm had}$ and $\Delta\alpha^{(5)}_{\rm had}(M_{\rm Z}^2)$ is evaluated using a parametrization of the ρ line shape based on vector resonances [10]. We obtain the additive corrections

$$\begin{aligned} \delta a_\mu^{\rm had} &= -(1.3 \pm 2.0) \times 10^{-10} \\ \delta\Delta\alpha^{(5)}_{\rm had}(M_{\rm Z}^2) &= -(0.09 \pm 0.12) \times 10^{-4} \end{aligned} \qquad (22)$$

for the $\tau^- \to \pi^-\pi^0\,\nu_\tau$ spectral function which is applied in the present analysis. Corrections from the higher mass resonances $\rho(1450), \rho(1700)$ are expected to be negligible.

The two- and four-pion cross sections (incl. the τ contribution) in different energy regions are depicted in Figs. 2 and 3. The bands are the results within (diagonal) error-envelopes of the averaging procedure and the application of the trapezoidal rule described in Sect. 2.

6.1 Lowest order hadronic contributions

The results of the exclusive contributions to a_μ^{had} and $\Delta\alpha^{(5)}_{\rm had}\ (M_{\rm Z}^2)$ are presented in Table 2. After the inclusion of the τ data, the error of a_μ^{had} is dominated much less by the uncertainty of the two-pion contribution.

Other important sources are the contradictory $\pi^+\pi^-2\pi^0$ data, as well as the unmeasured $\pi^+\pi^-4\pi^0$ final state. In the latter case, limits can be set only by using very conservative isospin arguments. As shown in [10] by means of a decomposition in orthogonal isospin classes (Pais [79]) the large upper limit comes from the assumption of a dominant σ_{411} class accompanied by a vanishing σ_{321} contribution. Both classes occur in $\pi^+\pi^-\pi^+\pi^-2\pi^0$, while none contributes to $\pi^+\pi^-\pi^+\pi^-\pi^+\pi^-$ and only σ_{411} is part of $\pi^+\pi^-4\pi^0$. The measured cross section of $\pi^+\pi^-\pi^+\pi^-2\pi^0$ is clearly higher than the corresponding $\pi^+\pi^-\pi^+\pi^-\pi^+\pi^-$ final state hence guaranteeing a leading contribution from one of the classes mentioned if isospin invariance holds. Since those classes correspond to eigenstates, a resonance analysis of the measured six-pion data would reveal important properties of the class structure of the respective modes which thus could give more constraining isospin bounds.

Another large uncertainty comes from the $K\bar{K}\pi\pi$ final states. The measurement of the $K^+K^-\pi^+\pi^-$ mode alone does not allow one to calculate isospin bounds for all possible contributions. Fortunately, it is possible to extract the complete $K\bar{K}\pi\pi$ contribution on the basis of a DM1 measurement of the inclusive channel K^0_S+X [58]. Nevertheless, large experimental uncertainties prevent a precise determination of the corresponding integrals.

The last important error source, especially for $\Delta\alpha^{(5)}_{had}(M_{\rm Z}^2)$, comes from the integral over the measured high energy inclusive cross section ratio R. The reliability of the QCD perturbative expansion for energies sufficiently above the still unpredictable resonance phenomena has been proven in many cases (see, *e.g.*, α_s measurements from different energy scales at LEP, HERA and from τ decays). Thus, theoretical input at energies lower than 40 GeV should be reliable and could significantly help to reduce the integration uncertainties [82,83]. However, this has not been used in the present analysis which relies on experimental data as far as possible.

The squared contributions of the various final states and energy regimes to the errors of a_μ^{had} and $\Delta\alpha(M_{\rm Z}^2)$ are depicted in Fig. 4. Only the results after the inclusion of τ data are shown.

Table 2. Summary of the a_μ^{had} and $\Delta\alpha^{(5)}_{had}(M_Z^2)$ contributions from e^+e^- annihilation and τ decays. The line "$\pi^+\pi^-$ threshold" contains the results from the integral over expression (21) at threshold energies

Final states	a_μ^{had} ($\times 10^{10}$)	$\Delta\alpha^{(5)}_{had}(M_Z^2)$ ($\times 10^4$)	Energy (GeV)
$\pi^+\pi^-$ threshold	2.30 ± 0.05	0.04 ± 0.00	$4m_\pi^2 - 0.320$
$\pi^+\pi^-$	495.86 ± 12.46	34.01 ± 0.87	0.320 – 2.125
$\pi^+\pi^-$ (incl. τ data)	500.81 ± 6.03	34.31 ± 0.38	0.320 – 2.125
$\rho(\pi^0\gamma + \eta\gamma)$ [1]	0.30 ± 0.05	0.02 ± 0.01	0.298 – 2.125
ω	37.09 ± 1.07	2.97 ± 0.09	0.420 – 0.810
$\omega \to \pi\gamma$, neutrals [1]	0.03 ± 0.01	< 0.01	0.810 – 2.125
ϕ	39.23 ± 0.94	5.18 ± 0.12	1.000 – 1.055
$\phi \to \eta\gamma$, $\pi^0\gamma$ [1]	0.09 ± 0.01	0.01 ± 0.00	1.055 – 2.125
$\pi^+\pi^-\pi^0$ (below ϕ)	4.12 ± 0.41	0.42 ± 0.04	0.810 – 1.000
$\pi^+\pi^-\pi^0$ (above ϕ)	1.90 ± 0.72	0.46 ± 0.26	1.055 – 2.125
$\pi^+\pi^-2\pi^0$	21.41 ± 2.36	5.82 ± 0.63	0.910 – 2.125
$\pi^+\pi^-2\pi^0$ (incl. τ data)	22.26 ± 1.53	6.16 ± 0.49	0.897 – 2.125
$\omega\,\pi^0(\omega \to \pi\gamma$, neutr.) [1]	0.88 ± 0.11	0.18 ± 0.02	0.930 – 2.125
$\pi^+\pi^-\pi^+\pi^-$	15.90 ± 1.34	4.61 ± 0.39	0.983 – 2.125
$\pi^+\pi^-\pi^+\pi^-$ (incl. τ data)	16.50 ± 0.98	4.76 ± 0.31	0.794 – 2.125
$\pi^+\pi^-\pi^+\pi^-\pi^0$	4.02 ± 0.51	1.51 ± 0.20	1.019 – 2.125
$\pi^+\pi^-3\pi^0$ [2]	2.01 ± 0.26	0.75 ± 0.10	1.019 – 2.125
$\omega\,\pi^+\pi^-(\omega \to \pi\gamma$, neutr.) [1]	0.07 ± 0.02	0.03 ± 0.01	1.340 – 2.125
$\pi^+\pi^-\pi^+\pi^-\pi^+\pi^-$	0.47 ± 0.14	0.19 ± 0.04	1.350 – 2.125
$\pi^+\pi^-\pi^+\pi^-2\pi^0$	3.32 ± 0.36	1.35 ± 0.14	1.350 – 2.125
$\pi^+\pi^-4\pi^0$ [2]	2.40 ± 2.40	0.98 ± 0.98	1.350 – 2.125
$\eta\,\pi^+\pi^-$ [3]	0.51 ± 0.14	0.16 ± 0.05	1.075 – 2.125
K^+K^-	4.30 ± 0.58	0.85 ± 0.10	1.055 – 2.055
$K^0_S K^0_L$	1.20 ± 0.42	0.23 ± 0.08	1.090 – 2.125
$K^0_S K^+\pi^-$ (+ $K^0_L K^-\pi^+$ [2])	2.04 ± 0.36	0.70 ± 0.12	1.340 – 2.125
$K^+K^-\pi^0$	0.42 ± 0.29	0.15 ± 0.10	1.440 – 2.125
$K^0_S K^0_L \pi^0$ [2]	0.42 ± 0.29	0.15 ± 0.10	1.440 – 2.125
$K\bar{K}\pi\pi$ (all modes)	4.52 ± 1.65	1.82 ± 0.66	1.441 – 2.125
J/ψ(1S,2S,3770)	8.04 ± 0.52	9.97 ± 0.68	3.096 – 3.800
Υ(1S,2S,3S,4S,10860,11020)	0.10 ± 0.01	1.18 ± 0.08	9.460 – 11.20
R	41.64 ± 3.61	164.31 ± 5.59	2.125 – 40.0
R (perturbative) [4]	0.16 ± 0.00	42.82 ± 0.10	40.0 – ∞
$\sum (e^+e^- \to$ hadrons)	695.0 ± 15.0	280.9 ± 6.3	$4m_\pi^2 - \infty$
$\sum (e^+e^- \to$ hadrons) (incl. τ data)	701.1 ± 9.4	281.7 ± 6.2	$4m_\pi^2 - \infty$

[1] Correction for missing modes (see text)
[2] Deduced from isospin relations (see text)
[3] Without contribution from $\eta \to \pi^+\pi^-\pi^0$ and $\eta \to 3\pi^0$
[4] Values are taken from [7]

We obtain for the lowest order hadronic vacuum polarization diagram of the muonic anomalous magnetic moment the contributions

$$a_\mu^{had} = (695.0 \pm 15.0) \times 10^{-10} \quad (e^+e^- \text{ data only})$$
$$a_\mu^{had} = (701.1 \pm 9.4) \times 10^{-10} \quad (\text{combined } e^+e^- \text{ and } \tau \text{ data})$$

and for the running of α at M_Z^2

$$\Delta\alpha^{(5)}_{had}(M_Z^2) = (280.9 \pm 6.3) \times 10^{-4} \quad (e^+e^- \text{ data only})$$
$$\Delta\alpha^{(5)}_{had}(M_Z^2) = (281.7 \pm 6.2) \times 10^{-4} \quad (\text{combined } e^+e^- \text{ and } \tau \text{ data}) .$$

Figure 5 shows a compilation of published results. The inclusion of the new τ data yields a large improvement

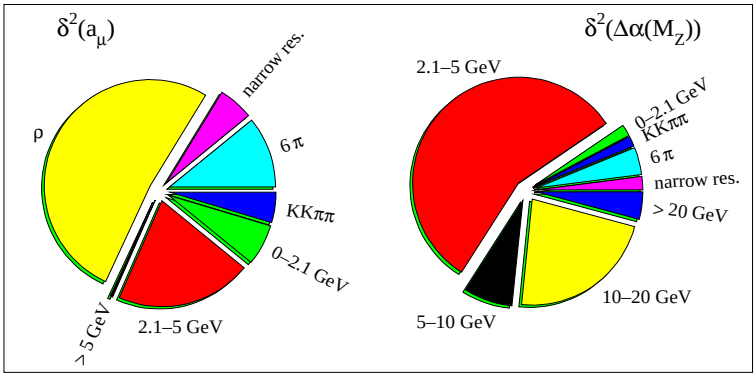

Fig. 4. Quadratic contribution of the various error sources to a_μ^{had} (*left hand plot*) and $\Delta\alpha^{(5)}_{had}(M_Z^2)$ (*right hand plot*) after the inclusion of τ data. In the energy region 0–2.1 GeV we include all exclusive contributions that are not given separately

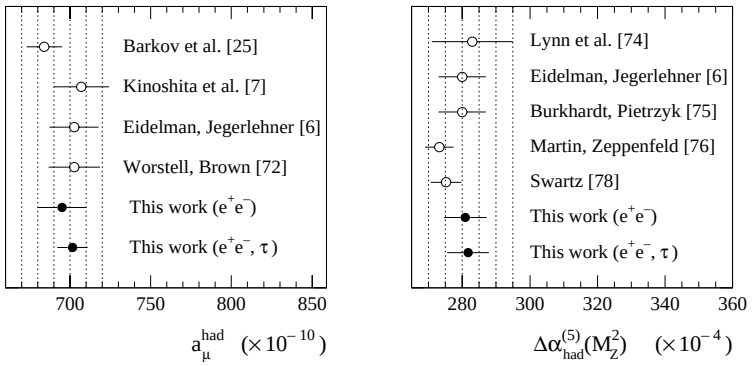

Fig. 5. Comparison of estimates of a_μ^{had} (lowest) and $\Delta\alpha^{(5)}_{had}(M_Z^2)$

in the precision of the a_μ^{had} determination. The difference in a_μ^{had} between the exclusive e^+e^- analyses of [7] and this work is mainly due to a disagreement in the two-pion integral where we obtain significantly lower values. In addition, differences in the handling of unmeasured modes generate inconsistent results. The results of [9] cannot easily be compared to the newer ones as the data set did not include the recent DM2 results. The differences in the final errors of a_μ^{had} in the exclusive e^+e^- analysis of this work compared to [7,78] is mainly caused by different techniques in the handling of the data and their errors. The detailed study of the origin of correlations, their propagation, as well as the rigourous use of isospin constraints to bound unmeasured modes yield slightly smaller errors here. As expected, the gain in the precision of a_μ^{had} coming from τ data is significant whereas it is very small for $\Delta\alpha^{(5)}_{had}(M_Z^2)$ since the dominant contributions and uncertainties come from energies above the τ mass.

6.2 Higher order contributions

In the famous paper of Kinoshita et al. [9], higher order contributions to the muon hadronic vacuum polarization graph, such as additional lepton or quark loops inserted in the diagram of Fig. 1 and the so-called light-by-light scattering graph, have been evaluated. The latter has been re-computed by different groups obtaining $(-5.2 \pm 1.8) \times 10^{-10}$ [85] and $(-9.2 \pm 3.2) \times 10^{-10}$ [86] with large uncertainties compared to the designed experimental accuracy of $\Delta a_\mu \simeq 4.0 \times 10^{-10}$ of the forthcoming BNL experiment. We use the value of $(-6.2 \pm 4.0) \times 10^{-10}$ in the following with an enlarged error to account for inconsistencies.

The calculation of the higher order $\mathcal{O}(\alpha/\pi)^3$ loop diagrams is accomplished and partly corrected in a recent work [87], where second order kernel functions $K^{(2)}(s)$ are provided. These are used to calculate the corresponding contributions in the same spirit as the dominant lowest order graph by virtue of the dispersion integral (6). The numerical evaluation in [87] was performed on the basis of the data sample used by [7]. We repeat this exercise here in order to check the consistency of the results. For the contribution of diagrams with additional photon exchanges, *e.g.*, the fourth order muon vertex correction, we use the kernel labeled $K^{(2a)}(s)$ in [87] and obtain $a_\mu^{(2a)} = (-20.9 \pm 0.4) \times 10^{-10}$. The diagrams with an electron loop inserted in one of the photon lines of Fig. 1 (kernel $K^{(2b)}(s)$ in [87]) contribute to $a_\mu^{(2b)} = (10.6 \pm 0.2) \times 10^{-10}$, where the asymptotic expansion, the analytical and numerical solutions provided in [87] lead to very similar results. Finally, the insertion of two hadronic loops in the muon vertex correction graph (kernel $K^{(2c)}(s)$ in [87]) results in $a_\mu^{(2c)} = (0.27 \pm 0.01) \times 10^{-10}$. The contributions $a_\mu^{(2a,b,c)}$ are found to be in agreement with [87]. All higher order results given here are computed from the e^+e^- data set only.

The compilation of the hadronic higher order parts (including light-by-light scattering) yields $a_\mu^{had}[(\alpha/\pi)^3] = (-16.2 \pm 4.0) \times 10^{-10}$.

6.3 Results for a_μ and $\alpha(M_Z^2)$

Collecting all contributions, we obtain for the anomalous magnetic moment of the muon

$$a_\mu = (11\,659\,164.5 \pm 15.6) \times 10^{-10}$$
$$(e^+e^- \text{ data only})$$
$$a_\mu = (11\,659\,170.6 \pm 10.2) \times 10^{-10}$$
$$(\text{combined } e^+e^- \text{ and } \tau \text{ data}) ,$$

where the errors of the lowest order calculation a_μ^{had} and $a_\mu^{(2a,b,c)}$ are added linearly.

The inverse of the fine structure constant at M_Z^2 is found to be

$$\alpha^{-1}(M_Z^2) = 128.889 \pm 0.087$$
$$(e^+e^- \text{ data only})$$
$$\alpha^{-1}(M_Z^2) = 128.878 \pm 0.085$$
$$(\text{combined } e^+e^- \text{ and } \tau \text{ data}) .$$

One may use the latter (combined) result for $\alpha(M_Z^2)$ to improve the constraint on the mass of the standard model Higgs boson $M_{\rm Higgs}$ inferred from a global electroweak fit. This is done by utilizing current available electroweak data [88,89] and the ZFITTER electroweak library [90]. It requires M_Z, $m_{\rm top}$, and $\alpha(M_Z^2)$ as input parameters, which are allowed to vary within their experimental accuracies. The additional parameters $M_{\rm Higgs}$ and the strong coupling constant at M_Z^2, $\alpha_s(M_Z^2)$, are freely adjusted in the fit. We obtain $\alpha_s(M_Z^2) = 0.1201 \pm 0.0033$ which is in perfect agreement with the experimental value of 0.122 ± 0.006 [91] from the analyses of QCD observables in hadronic Z decays at LEP. The fitted Higgs boson mass is 138^{+137}_{-76} GeV, compared to 149^{+148}_{-82} GeV when using the previous value of $\alpha(M_Z^2)$ from (13). An additional error of 50 GeV should be added to account for theoretical uncertainties [90].

Figure 6 depicts the variation of χ^2 as a function of the Higgs boson mass for the new and previously used values of $\alpha(M_Z^2)$ (the latter taken from [7]). We obtain an upper limit for $M_{\rm Higgs}$ of 516 GeV at 95% CL.

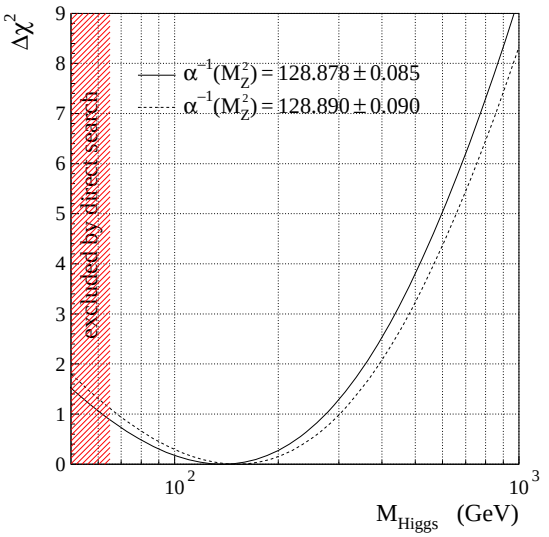

Fig. 6. Constraint fit results for the previous and the new value of $\alpha(M_Z^2)$ as a function of the Higgs mass

7 Conclusions

We have reevaluated the hadronic vacuum polarization contribution to $(g-2)$ of the muon and to the running of the QED fine structure constant $\alpha(s)$ at $s = M_Z^2$. We used new data from τ decays, recently published by the ALEPH Collaboration, in addition to slightly enlarged e^+e^- annihilation cross section data sets in order to improve the precision of the corresponding integrals. Our results are, to lowest order, $a_\mu^{had} = (701.1 \pm 9.3) \times 10^{-10}$ yielding $a_\mu = (11\,659\,170.6 \pm 10.2) \times 10^{-10}$ and $\Delta\alpha^{(5)}_{had}(M_Z^2) = (281.7 \pm 6.2) \times 10^{-4}$, propagating $\alpha^{-1}(0)$ to $\alpha^{-1}(M_Z^2) = (128.878 \pm 0.085)$. The improvement coming from τ data is small in the $\Delta\alpha^{(5)}_{had}(M_Z^2)$ case which is dominated by high energy contributions. However, it causes a 37% reduction in the error on a_μ^{had}.

In the near future, new low energy e^+e^- annihilation data are expected to be produced by the CMD-2 Collaboration [11] at Novosibirsk. In addition, new results for the $\tau^- \to \pi^-\pi^0\,\nu_\tau$ spectral function with a precision comparable to the ALEPH data were recently presented by the CLEO Collaboration [92]. Significant improvement is also expected from energy scans at the future high-luminosity e^+e^- collider DAΦNE in Frascati.

Acknowledgements. It is a pleasure to thank A. Blondel, H. Burkhardt, S. Eidelman, L. Duflot, M. Finkemeier, F. Jegerlehner, B. Krause, W. Marciano, A. Pich, B. Pietrzyk, P. Singer and F. Teubert for helpful comments and interesting discussions. We are indebted to S. Sen for carefully reading this manuscript.

References

1. J. Bailey et al., Phys. Lett. **B68** (1977) 191
   F.J.M. Farley and E. Picasso, 'The muon $(g-2)$ Experiments', Advanced Series on Directions in High Energy Physics - Vol. 7 Quantum Electrodynamics, ed. T. Kinoshita, World Scientific 1990
2. B. Lee Roberts, Z. Phys. **C56** (Proc. Suppl.) (1992) 101. See also http://www.phy.bnl.gov/g2muon/home.html
3. A. Czarnecki, B. Krause and W.J. Marciano, Phys. Rev. Lett. **76** (1995) 3267; Phys. Rev. **D52** (1995) 2619
4. T.V. Kukhto, E.A. Kuraev, A. Schiller and Z.K. Silagadze, Nucl. Phys. **B371** (1992) 567
5. R. Jackiw and S. Weinberg, Phys. Rev. **D5** (1972) 2473
6. S. Peris, M. Perrottet and E. de Rafael, Phys. Lett. **B355** (1995) 523
7. S. Eidelman and F. Jegerlehner, Z. Phys. **C67** (1995) 585
8. C. Bouchiat and L. Michel, J. Phys. Radium **22** (1961) 121

9. T. Kinoshita, B. Nižić and Y. Okamoto, Phys. Rev. **D31** (1985) 2108.
10. D. Buskulic et al. (ALEPH Collaboration), CERN PPE/97-013 (1997)
11. S. Eidelman, Talk given at the TAU'96 Conference, Colorado 1996
12. S. Tisserant and T.N. Truong, Phys. Lett. **B115** (1982) 264;
A. Pich, Phys. Lett. **B196** (1987) 561;
H. Neufeld and H. Rupertsberger, Z. Phys. **C68** (1995) 91
13. R.M. Barnett et al. (Particle Data Group), Phys. Rev. **D54** (1996) 1
14. W.K. McFarlane et al., Phys. Rev. **D32** (1985) 547
15. P. Singer, Phys. Rev. **130** (1963) 2441; Erratum: **161** (1967) 1694
16. J. Bijnens and P. Gosdzinsky, **Phys. Lett. B388** (1996) 203
17. J. Gasser and H. Leutwyler, Phys. Rep. **87** (1982) 77
18. E. Braaten and C.S. Li, Phys. Rev. **D42** (1990) 3888
19. E. Braaten, S. Narison and A. Pich, Nucl. Phys. **B373** (1992) 581
20. W.J. Marciano and A. Sirlin, Phys. Rev. Lett. **56** (1986) 22; Phys. Rev. Lett. **61** (1986) 1815
21. R. Decker and M. Finkemeier, Nucl. Phys. **B438** (1995) 17
22. M. Finkemeier, W. Marciano and A. Pich, private communications (Nov. 1996)
23. M. Gourdin and E. de Rafael, Nucl. Phys. **B10** (1969) 667
24. S.J. Brodsky and E. de Rafael, Phys. Rev. **168** (1968) 1620
25. N. Cabbibo and R. Gatto, Phys. Rev. Lett. **4** (1960) 313; Phys. Rev. **124** (1961) 1577
26. S.G. Gorishny, A.L. Kataev and S.A. Larin, Phys. Lett. **B259** (1991) 144;
L.R. Surguladze and M.A. Samuel, Phys. Rev. Lett. **66** (1991) 560
27. G. D'Agostini, Nucl. Inst. Meth. **A346** (1994) 306
28. G.J. Gounaris and J.J. Sakurai, Phys. Rev. Lett. **21** (1968) 244
29. S. Jadach, J.H. Kühn and Z. Wąs, Comp. Phys. Comm. **64** (1991) 275;
S. Jadach, B.F.L. Ward and Z. Wąs, Comp. Phys. Comm. **79** (1994) 503;
S. Jadach et al., Comp. Phys. Comm. **76** (1993) 361
30. D. Buskulic et al. (ALEPH Collaboration), Z. Phys. **C70** (1996) 579
31. L.M. Barkov et al. (OLYA, CMD Collaboration), Nucl. Phys. **B256** (1985) 365
32. I.B. Vasserman et al. (OLYA Collaboration), Sov. J. Nucl. Phys. **30** (1979) 519
33. I.B. Vasserman et al. (TOF Collaboration), Sov. J. Nucl. Phys. **33** (1981) 709
34. S.R. Amendolia et al. (NA7 Collaboration), Phys. Lett. **B138** (1984) 454
35. A. Quenzer et al. (DM1 Collaboration), Phys. Lett. **B76** (1987) 512
36. D. Bisello et al. (DM2 Collaboration), Phys. Lett. **B220** (1989) 321
37. S.J. Dolinsky et al. (ND Collaboration), Phys. Rep. **C202** (1991) 99
38. G. Cosme et al. (M2N Collaboration), Phys. Lett. **B63** (1976) 349;
G. Parrour et al. (M2N Collaboration), Phys. Lett. **B63** (1976) 357
39. G. Cosme et al. (M3N Collaboration), Nucl. Phys. **B152** (1979) 215;
C. Paulot, Thesis, LAL-79-14, Orsay (1979)
40. A. Cordier et al. (DM1 Collaboration), Nucl. Phys. **B172** (1980) 13
41. A. Antonelli et al. (DM2 Collaboration), Z. Phys. **C56** (1992) 15
42. L.M. Kurdadze et al. (OLYA Collaboration), JETP Lett. **43** (1986) 643
43. D. Bisello (for the DM2 Collaboration), Nucl. Phys. **B21** (Proc. Suppl.) (1995) 111
44. M. Schioppa (DM2 Collaboration), Thesis, Universita di Roma "La Sapienza" (1986)
45. D. Bisello et al. (DM2 Collaboration), Report LAL-90-35, Orsay (1990)
46. L. Stanco (for the DM2 Collaboration), Proceedings of Hadron-91 (World Scientific ed. 1992) 84
47. B. Esposito et al. (MEA Collaboration), Lett. Nuovo Cim. **28** (1980) 195
48. L.M. Barkov et al. (CMD Collaboration), Sov. J. Nucl. Phys. **47** (1988) 248
49. A. Cordier et al. (DM1 Collaboration), Phys. Lett. **B109** (1981) 155
50. A. Cordier et al. (DM1 Collaboration), Phys. Lett. **B81** (1979) 389
51. A. Antonelli et al. (DM2 Collaboration), Phys. Lett. **B212** (1988) 133
52. D. Bisello et al. (DM1 Collaboration), Phys. Lett. **B107** (1981) 145
53. P.M. Ivanov et al. (OLYA Collaboration), Phys. Lett. **B107** (1981) 297;
P.M. Ivanov et al. (OLYA Collaboration), JETP. Lett. **36** (1982) 112
54. D. Bisello et al. (DM1 Collaboration),
Reports LAL-80-35, LAL-80-36, LAL-80-37, Orsay (1980)
55. D. Bisello et al. (DM2 Collaboration), Z. Phys. **C39** (1988) 13
56. A. Cordier et al. (DM1 Collaboration), Phys. Lett. **B110** (1982) 335
57. F. Mané et al. (DM1 Collaboration), Phys. Lett. **B112** (1982) 178
58. F. Mané (DM1 Collaboration), Thesis, Université de Paris-Sud, LAL 82/46 (1982)
59. C. Bacci et al. ($\gamma\gamma 2$ Collaboration), Phys. Lett. **B86** (1979) 234
60. J.L. Siegrist et al. (MARK I Collaboration), Phys. Rev. **D26** (1982) 969
61. W. Bacino et al. (DELCO Collaboration), Phys. Rev. Lett. **40** (1978) 671
62. R. Brandelik et al. (DASP Collaboration), Phys. Lett. **B76** (1978) 361;
H. Albrecht et al. (DASP Collaboration), Phys. Lett. **B116** (1982) 383
63. J. Burmester et al. (PLUTO Collaboration), Phys. Lett. **B66** (1977) 395;
C. Berger et al. (PLUTO Collaboration), Phys. Lett. **B81** (1979) 410;
L. Criegee and G. Knies (PLUTO Collaboration), Phys. Rep. **C83** (1982) 151

64. B. Niczyporuk et al. (LENA Collaboration), Z. Phys. **C15** (1982) 299
65. Z. Jakubowski et al. (Crystal Ball Collaboration), Z. Phys. **C40** (1988) 49;
C.Edwards et al. (Crystal Ball Collaboration), SLAC-PUB-5160 (1990)
66. A.E. Blinov et al. (MD-1 Collaboration), Z. Phys. **C49** (1991) 239;
A.E. Blinov et al. (MD-1 Collaboration), Z. Phys. **C70** (1996) 31
67. H.J. Behrend et al. (CELLO Collaboration), Phys. Lett. **B183** (1987) 400
68. W. Bartel et al. (JADE Collaboration), Phys. Lett. **B129** (1983) 145;
W. Bartel et al. (JADE Collaboration), Phys. Lett. **B160** (1985) 337;
B. Naroska (JADE Collaboration), Phys. Rep. **C148** (1987) 67
69. B. Adeva et al. (MARK-J Collaboration), Phys. Rev. Lett. **50** (1983) 799;
B. Adeva et al. (MARK-J Collaboration), Phys. Rev. Lett. **50** (1983) 2051;
B. Adeva et al. (MARK-J Collaboration), Phys. Rep. **C109** (1984) 131;
B. Adeva et al. (MARK-J Collaboration), Phys. Rev. **D34** (1986) 681
70. R. Brandelik et al. (TASSO Collaboration), Phys. Lett. **B113** (1982) 499;
M. Althoff et al. (TASSO Collaboration), Phys. Lett. **B138** (1984) 441
71. R. Giles et al. (CLEO Collaboration), Phys. Rev. **D29** (1984) 1285;
D. Besson et al. (CLEO Collaboration), Phys. Rev. Lett. **54** (1985) 381
72. E. Rice et al. (CUSB Collaboration), Phys. Rev. Lett. **48** (1982) 906
73. E. Fernandez et al. (MAC Collaboration), Phys. Rev. **D31** (1985) 1537
74. H. Burkhardt, F. Jegerlehner, G. Penso and C. Verzegnassi, Z. Phys. **C42** (1989) 497
75. J. Gasser and U.G. Meissner, Nucl. Phys. **B357** (1991) 90
76. S.R. Amendolia et al. (NA7 Collaboration), Nucl. Phys. **B277** (1986) 168
77. G. Colangelo, M. Finkemeier and R. Urech, Phys. Rev. D54 (1996) 4403
78. D.H. Brown and W.A. Worstell, Phys. Rev. **D54** (1996) 3237
79. A. Pais, Ann. Phys. **9** (1960) 548
80. B.W. Lynn, G. Penso and C. Verzegnassi, Phys. Rev. **D35** (1987) 42
81. H. Burkhardt and B. Pietrzyk, Phys. Lett. **B356** (1995) 398
82. A.D. Martin and D. Zeppenfeld, Phys. Lett. **B345** (1995) 558
83. K. Adel and F.Y. Ynduráin, FTUAM 95-32, hep-ph/9509378 (1995)
84. M.L. Swartz, Phys. Rev. **D53** (1996) 5268
85. M. Hayakawa, T. Kinoshita and A.I. Sanda, Phys. Rev. **D54** (1996) 3137; M. Hayakawa, T. Kinoshita and A.I. Sanda, Phys. Rev. Lett. **75** (1995) 790
86. J. Bijnens, E. Pallante and J. Prades, Nucl. Phys. **B474** (1996) 379
87. B. Krause, Phys. Lett. **B390** (1997) 392
88. A. Blondel, Talk given at the International Conference on High Energy Physics, Warsaw 1996
89. LEP Electroweak Working Group and the SLD Heavy Flavor Group, CERN LEPEWWG 96-02
90. 'Reports of the working group on precision calculations for the Z resonance', Ed. D. Bardin et al., CERN-PPE 95-03
91. S. Bethke, Talk given at QCD96, Montpellier 1996
92. J. Urheim (for the CLEO Collaboration), 'Spectral Functions of $\tau^- \to \pi^-\pi^0\,\nu_\tau$ and $\bar{\mathrm{K}}^0\pi^-\,\nu_\tau$', Talk given at the TAU'96 Conference, Colorado, 1996